

DEVELOPMENT OF A TERRA ROSSA SOIL PROFILE ON MARBLES OF THE CAMBRIAN NORMANVILLE GROUP AT DELAMERE, SOUTH AUSTRALIA



JORDAN FOSTER

HONOURS 2003

DEPARTMENT OF GEOLOGY & GEOPHYSICS, ADELAIDE UNIVERSITY

SUPERVISORS: DR. DAVID CHITTLEBOROUGH & DR. KARIN BAROVICH

Contents

Summary	Page 2
Introduction	Page 2
Geology & Landscape	Page 4
Methods	Page 4
Results	Page 6
<i>Morphological analysis</i>	
<i>Particle size analysis</i>	
<i>Mineralogical analysis</i>	
<i>Coarse particle morphology and elemental chemistry</i>	
Discussion	Page 10
<i>Micromorphology</i>	
<i>Particle size distribution and chemistry</i>	
<i>Clay and silt mineralogy</i>	
<i>Coarse particle morphology and elemental chemistry</i>	
Conclusion	Page 14
References	Page 14
Tables	Page 17
<i>Table 1 – Properties of the fine earth and insoluble residue</i>	
<i>Table 2 – X-ray fractionation data for trace element analysis</i>	
<i>Table 3 – X-ray fractionation data for major element analysis</i>	
<i>Table 4 – FESEM mineralogy counts of 125-2000μm fraction</i>	
Figure Captions	Page 23

Development of a Terra Rossa soil profile on marbles of the Cambrian Normanville Group at Delamere, South Australia

J. FOSTER

Department of Geology and Geophysics, School of Earth and Environmental Sciences, Adelaide University, Adelaide SA 5005

Summary

The genesis of Terra Rossa soils is still a matter of controversy. The two leading theories are: (1) that the soil is derived from the insoluble residue of the underlying limestone; or, (2) that contributions from some outside source account for large portions of the soil. Through morphological, analytical and mineralogical studies of a Terra Rossa soil profile at Delamere, South Australia, the insoluble residue of the underlying dolomite and a texture contrast profile from upslope, the major contributors to the soils development were determined. Also, field emission scanning electron microscopy (FESEM) of the coarse sand fraction was employed to determine the origin of coarse quartz grains in the soils. The Terra Rossa was discovered to be receiving considerable contributions from upslope via creep and/or colluvial movement, a feature that was most apparent in the upper horizons of the profile. The deeper horizons, however, appear to be largely derived from the insoluble residue of the dolomite, indicated by the mineralogy, particle size distribution, micromorphology and quartz grain morphology.

Introduction

Terra Rossa soils are common in areas with a Mediterranean climate (ie. cool, wet winters alternating with warm, dry summers). Soils in such climates have a xeric moisture regime (Soil Survey Staff, 1975). They characteristically overlie hard calcareous bedrock such as crystalline limestone or marble or unconsolidated calcareous deposits of terrestrial or marine origin (Kubiena, 1953). The genesis of these highly structured, uniform textured red soils has been a matter of controversy. Two hypotheses have prevalence: (1) in the 'residual theory' the development of the Terra Rossas are the result of

carbonate dissolution and subsequent accumulation and transformation of limestone residue (Bronger & Bruhn-Lobin, 1997). Gal (1967) and Moresi & Mongelli (1988) also subscribe to this explanation; and, (2) the other hypothesis is that the soil is unrelated to the underlying rock and is allochthonous in origin. For example aeolian dust is commonly posited as the parent material of red soils in the Mediterranean region (MacLeod, 1980; Yaalon, 1997).

Preliminary fieldwork in the southern and central Mount Lofty Ranges reveals a morphologically similar group of Terra Rossa soils over thin, elongate marble lenses of the lower Cambrian Normanville Group. Although Terra Rossa soils of South Australia have been studied (McIntyre, 1956; Norrish & Rogers, 1956; Stace, 1956), researchers have focused on regions other than the southern Fleurieu Peninsula and have been mainly concerned with mineralogical development. This region, however, provides an ideal scenario in which to test the hypotheses stated above. First, preliminary examination suggests that the marbles of the Normanville Group are quite pure, i.e. they have little argillaceous material. Large thicknesses of parent material would need to be weathered to account for the thickness of the solum. In a study of the genesis of a Terra Rossa in Epirus, Greece (MacLeod, 1980) calculated that for 40 cm of soil to develop, of the order of 130 m of limestone would need to be weathered. Given Yaalon & Ganor's (1975) calculation of 1-2 cm per 10^3 years for limestone denudation in Judea and Galilee, MacLeod (1980) suggested that the amount of residue released from limestone during denudation must accumulate at a rate of $8 \times 10^{-6} \text{ cm.a}^{-1}$ for 5×10^6 years. Even the oldest surfaces of the Delamere region are much younger than this (Wellman & Greenhalgh, 1988). Should such estimates apply here, given the tectonic instability of the Adelaide Geosyncline (Webb, 1957; Firman, 1969; Wellman & Greenhalgh, 1988), it is unlikely that a soil formed during the Tertiary could survive erosion. This would imply that the residual theory is an unlikely explanation.

Second, the marble lenses are found side by side with shales of the Normanville Group on which brown podsollic soils with strong texture contrast have developed. The transition between soil types is quite abrupt and seems coincident with lithological change. This implies that lithology is the dominant influence on the soil type and that the accession of material from upslope and/or aeolian deposition also seems an unlikely explanation.

The purpose of the study reported here was to establish the relationship of Terra Rossa soil to the underlying dolomite and the extent and origin of outside influences. Analytical tools include

morphological study of the soils, X-ray diffraction and X-ray fluorescence analysis of soil fractions and field emission scanning electron microscopy.

Geology and landscape

The lithology of the Delamere region is sandstones, siltstones and carbonates of the Cambrian Kanmantoo and Normanville Groups that belong to the Adelaidean sequence (Preiss, 1987), as well as the Permo-Carboniferous glacial deposits of the Cape Jervis Formation (Bourman & Alley, 1988). Terra Rossa soils are found overlying the hard Cambrian marbles/dolomites known as the Angaston Marble which is a member of the Normanville Group (Figure 1).

Much of the region has undergone deforestation, although there are large areas of blue gum woodland still intact. The site of the study has solely a grass cover and is currently used for grazing of cattle. Undulating rises and low hills with slopes between 10 and 30%, characterise the landform.

Delamere is located on the Fleurieu Peninsula approximately 100 km south of Adelaide. The annual mean minimum temperatures are between 9-12° C and the corresponding maximum temperatures between 18-21° C. Average annual rainfall is between 400 and 900 mm. The mean number of rainy days per year is 126.5 (Commonwealth Bureau of Meteorology, 2003). The climate - cool wet winters with excess water, alternating with warm dry summers – produces a xeric moisture regime in the soil profile.

Methods

Preliminary mapping and sampling of soil types in the area led to the identification of several possible sites for the study. These were selected on the ease of access and the extent and uniformity of the Terra Rossa. Core samples were taken at the northern most sample area (Figure 1) to determine the best place to collect bulk samples. The cores were taken using a rig attached to a 4WD, by traversing the landscape NW to SE, the Terra Rossa and adjacent soils were sampled. On the basis of recent soil-landscape mapping of Primary Industries and Resources South Australia, field inspections were made at the southernmost site of the marble outcrop (Figure 1). Using a backhoe, two trenches were dug, one in the Terra Rossa and the other in a Brown Podsollic soil of strong texture contrast from further upslope (Figure 2). Hereafter this soil profile will be referred to as the Upslope Soil. Following the photography of the

profiles 1-2 kg bulk samples of each horizon to bedrock were collected from the face of the trench. Sampling depths were based on changes in colour and texture down the profile.

Large undisturbed clods of soil were collected for micromorphological analysis. Sections of soil were carefully excised and packed for transport to the Canberra laboratories of CSIRO Land and Water where they were impregnated under vacuum with a polyester resin by the standard method of Brewer (1976). The impregnated blocks of soil were then sectioned to produce 7.5×5 cm slides for micromorphological analysis. Fabric and mineralogy were observed and photographed using a Leitz under polarized light according to the method of Brewer & Sleeman (1988).

The morphologies of the profiles were described using the Munsell colour system, along with methods outlined in McDonald *et al.* (1984) for texture and structure (Figures 3 & 4).

Separation of the fine earth (<2000 μ m) into clay (<2 μ m), silt (2-20 μ m), very fine sand (20-53 μ m), fine sand (53- 125 μ m) and coarse sand (125-2000 μ m) fractions was carried out by sedimentation and sieving. The insoluble residue of the dolomite was obtained through dissolution via 0.5M HCl solution. The same process allowed the calculation of the percentage of insoluble residue by comparing the initial and final weights of the material. The residue was separated following the same procedure as that described above.

Cation exchange capacity was measured using the alcoholic ammonium chloride procedure based on the method described by Rayment & Higgson (1992). Exchangeable bases were determined using atomic absorption for calcium and magnesium and flame photometry for potassium and sodium.

Electrical conductivity and pH were measured in a solution of 8 g of sample and 40 mL of water.

Major elemental analysis was conducted using a Philips PW 1480 X-ray Fluorescence Spectrometer with a dual-anode (Sc-Mo) x-ray tube operating at 40kV, 75mA at the Department of Geology and Geophysics, Adelaide University. Samples were prepared by drying for 2 hours at 110° C to remove moisture; transferring the soil into alumina crucibles and igniting overnight at 960° C in order to obtain loss on ignition (LOI) values. 1 g of ignited sample and 4 g of flux were fused using a propane-oxygen flame (at approximately 1150° C) and cast into a preheated Pt-Au mould to produce a glass disc suitable for analysis. Analysis of the trace elements was also conducted using a Philips PW 1480 Fluorescence Spectrometer. Preparation of the samples required approximately 5 g of sample, using boric acid as a backing, to be pressed into pellet form for analysis.

Oriented disks were prepared for x-ray diffraction by pipetting a suspension of clays, under suction, onto Ag filters of pore size $0.45\mu\text{m}$. Clays were saturated with 1M MgCl_2 , washed free of excess electrolyte and saturated with 10% glycerol. X-ray diffractograms were generated using a Philips PW 1800 microprocessor-controlled diffractometer with $\text{CoK}\alpha$ radiation, variable divergence slit and a graphite monochromator. Patterns were acquired from 3 to $33^\circ 2\theta$ in 0.02° steps and analysed using the software program X-Plot. A sample from the silt fraction of the Terra Rossa from depth 40-47cm received treatment with 1M KCl and 5% glycerol to determine the presence of vermiculite.

Mineral types and morphology of grains in the coarse sand fractions were observed using a Philips XL30 Field Emission Scanning Electron Microscope (FESEM) with the acceleration voltage set to 20kV. The samples were fixed to the sample holder with double-sided tape and a carbon coating was applied prior to analysis. Mineralogical analysis conducted with the FESEM required use of the EDAX program iDXI(maps). The concentrations of elements in each grain were measured by EDAX. The mineralogy of each grain was assigned manually by scanning its elemental distribution. Each sample was analysed in 56 fields. Within each field iDXI(maps) distinguished individual grains and, using x-rays, determine the elements present. Due to the volume of data, the mineralogy of each sample was determined from only 5 randomly selected fields out of a possible 56.

Results

Morphological analysis

The Terra Rossa profile is dark reddish brown with hues ranging from 2.5YR to 5YR (YR: yellow/red hue). The C horizon (weathered bedrock) is strong brown with a hue of 7.5YR and is distinctly calcareous in contrast to the A and B horizons that contain no noticeable carbonate. The profile has a strong subangular to angular blocky structure and medium texture (clay loam) throughout (Figure 3). The soil is a gradational clay loam and a Red Dermosol (Isbell, 1996).

The upslope profile is dark reddish brown to very dark brown in the A and upper B horizons and strong to light brown in the lower B and C horizons. The hues range from 5YR in the A to 10YR in the C horizon. There is a strong texture contrast between A and B horizons unlike the texture of the Terra Rossa profile that is more uniform throughout (Figure 4). The soil is a loam over brown clay and a Eutrophic, Brown Chromosol (Isbell, 1996).

Micromorphological analysis of the soils under thin section shows the Terra Rossa to have an iron-rich, aseptic plasmic fabric i.e. the clay particles are highly flocculated, demonstrating no visible clay separations. It also demonstrates a high degree of microraggregation of particles. The dolomite has highly variable particle sizes that occur as bands of like sized grains through the rock and contains argillaceous material in stylolites. The upslope profile shows evidence of considerable clay mobility, with the formation of argillans in cracks and vughs.

Particle size analysis (Table 1)

The Terra Rossa fine earth is dominated by the clay fraction, with lesser amounts of the silt and very fine sand fractions. The lower two horizons show the greatest clay content and contain very little else of the fine earth. The A horizon has less clay but higher silt and very fine sand than the rest of the profile (Figure 5a).

Dissolution of 510.25 g of dolomite yielded 33.53 g of insoluble residue: hence the dolomite consists of approximately 6.5% insoluble residue that is predominantly sand (86%) composed of very fine sand (21%), fine sand (33%) and coarse sand (22%), values that are considerably greater than the solum. The clay fraction accounts for only 6% of the total fine earth.

The Upslope profile is principally clay, silt and very fine sand. Whereas in the A horizon (0-10 cm) these fractions are roughly equal, the deeper horizons have considerably more clay (Figure 5b).

In comparison, the Terra Rossa horizons contain larger percentages of clay than their Upslope counterparts. The opposite is true for the silt, very fine sand and fine sand fractions, whereas the coarse sand fractions are quite similar (Figure 5).

The $\text{Al}_2\text{O}_3:\text{Fe}_2\text{O}_3$ ratios (Figure 6a) from the whole soil samples reveal a greater relative proportion of Fe_2O_3 in the Terra Rossa than the Upslope soil. The Terra Rossa $\text{Al}_2\text{O}_3:\text{Fe}_2\text{O}_3$ ratio decreases with depth indicating a relative increase in Fe_2O_3 . The values also show less difference between horizons down the profile. While relative Fe_2O_3 decreases up the profile for both soil types, the highest ratio of $\text{Al}_2\text{O}_3:\text{Fe}_2\text{O}_3$ in the Terra Rossa (2.25) is still smaller than the lowest value of the Upslope profile (2.35).

The $\text{Al}_2\text{O}_3:\text{K}_2\text{O}$ ratios (Figure 6b) of the Terra Rossa soil show a decrease in relative K_2O with depth, in particular a marked difference between 20-28 cm (6.6) and 40-47 cm (10.6). The dolomite itself, however, shows a significant increase in K_2O relative to Al_2O_3 . The Upslope profile also shows a relative decrease in K_2O with depth, with only a slight increase in the parent rock.

The ratio $K_2O:CaO$ (Figure 6c) reveals greater amounts of K_2O in the upper section of the profile (0-10 cm & 20-28 cm), however at 40-47 cm relative CaO increases significantly and continues to with depth. The Upslope profile has a considerable increase in K_2O relative to CaO with depth.

$K_2O:SiO_2$ (Figure 6d) shows little change with depth in the Terra Rossa, the dolomite however has significantly more K_2O relative to SiO_2 than the rest of the profile. The Upslope profile increases in relative K_2O with depth.

The ratio of $Fe_2O_3:K_2O$ (Figure 6e) from the Terra Rossa profile increases with depth, showing a significant jump between 20-28 cm (3.3) and 40-47 cm (5.6). The dolomite, however, has a smaller $Fe_2O_3:K_2O$ ratio than any sample from its overlying soil. The Fe_2O_3 increases relative to K_2O from the A to the B horizon in the Upslope profile, then decreases from the B horizon to the parent rock.

The $TiO_2:Zr$ ratio (Figure 6f) increases with depth, but there is a significant relative increase in Zr in the dolomite. Between 20-28 cm (3.4) and 40-47 cm (4.2) the level of Ti suddenly increases. There is a significant increase between the ratio of the A horizon (0-10 cm) and the B horizon (42-63 cm) of the Upslope profile. The B horizon and the parent rock show no change.

Mineralogical analysis

XRD analysis of the silt (2-20 μm) fraction (Figure 7a) of the Terra Rossa profile reveals a dominance of quartz and primary mica. The sharp peaks of these minerals suggest they have strong crystallinity. Whereas only a small amount of quartz exists in the marble itself, it increases considerably up the profile and reaches its greatest abundance in the A horizon (0-10 cm). The lower B horizon (40-47 cm) contains a substantial amount of well-ordered vermiculite (Figure 8a) that is missing in the insoluble residue and the A and upper B horizons.

The Terra Rossa clay (<2 μm) fraction (Figure 9a) consists of poorly-ordered mica that shows greater crystallinity higher up the profile. Poorly-crystalline kaolinite is present as indicated by the broad peaks that may also indicate illite-kaolinite intergrades (Figure 10a). Quartz again shows an increase up the profile. There is little in the dolomite and the horizon immediately above it, but quartz is present in the upper horizons.

Analysis of the Upslope profile reveals that in the silt fraction, primary mica and quartz are the only minerals present in the A horizon (Figure 7b). A small peak in the B horizon shows what may be the

beginnings of the breakdown of mica to vermiculite with a bridge between the two peaks indicating intergrading of mica and vermiculite (Figure 8b).

The mineralogy of the clay fraction is largely kaolinite and quartz (Figure 9b). Quartz increases up the profile and is dominant in the A (0-10 cm) and B1 (23-42 cm) horizons, whereas poorly ordered kaolinite is the dominant mineral in the lower horizons. Halloysite is present as indicated by the slope on the low angle side of the first order kaolinite peak (Figure 10b).

Coarse particle morphology and elemental chemistry (Table 4 & Figure 11)

The FESEM analysis of the coarse sand (125-2000 μ m) fraction reveals mica to be the dominant mineral (61%) in the insoluble residue. The mica is present as well-ordered crystals (Figure 11d). Quartz is present in large quantities (38%). Potassium feldspar makes up a small portion (1%) of this fraction (Table 4). Quartz grains are highly pitted, a morphology indicative of dissolution of silica (Figure 11e). Dissolution of silica is consistent with the highly alkaline conditions associated with chemical weathering of carbonate (Dove & Nix, 1997).

Mica (50%) is the dominant mineral of the Terra Rossa B horizon (20-28 cm). Quartz and K feldspar are also present in considerable quantities (30 and 20% respectively). The mica in this horizon does not show the same degree of crystallinity as that in the insoluble residue, appearing largely as hydrated mica particles that show a great deal of alteration due to water (Figure 11b). The weathering results in decreased crystallinity of the mica. The quartz grains are generally smooth and subrounded to well-rounded with a few pits and grooves. A few show evidence of extensive dissolution but the proportion of grains showing this feature is much less than in the dolomite.

The A horizon is largely quartz (65%), and the concentration of mica is 32%. K feldspar is also present in small amounts (3%).

The B horizon shows a significant increase in quartz (70%) relative to mica (18%) and K feldspar (12%). There is a considerable increase in quartz (82%) in the A horizon: mica (8%) and K feldspar (10%) are in minor proportions.

In the C horizon (85-100 cm) of the Upslope profile quartz, feldspar and mica are co-dominant.

The morphology of the grains from the Upslope profile remains the same throughout. The quartz and feldspar grains are subrounded to well-rounded, with some pits and grooves (Figures 11f, h & j). This

morphology contrasts sharply with that of the grains in the dolomite that are strongly pitted and etched. Mica is present in hydrated form only (Figures 11g & i).

Discussion

Micromorphology

The strong structure, characteristic of the Terra Rossa profile, is due to high Ca (Table 1) released from the dolomite during dissolution and which the clays take up as an exchangeable cation. High flocculation of particles due to the Ca, as well as Fe-oxide and organic matter, inhibits the movement of clay through the profile, suggesting clay illuviation should not be evident in the Terra Rossa profile (Bartelli & Odell, 1960). This is not supported by the fractionation data that shows a relative increase in clay sized particles from the A to the B horizon (Figure 5a).

The high mobility of clay in the Upslope profile suggests that clay illuviation is taking place. Less Ca in the Upslope profile means that clay particles are free to move through the profile. The greater proportion of clay sized particles in the B horizon than the A supports this (Figure 5b).

A likely explanation for the greater proportion of silt and sand sized particles in the A horizon of the Terra Rossa is that soil creep and/or colluviation of the coarser grained upper horizons of the Upslope soil is reducing the concentration of clay in the upper Terra Rossa profile. Although clay is present in the Upslope A horizon and is likely to be transported with the coarser material the extent to which it contributes to the Terra Rossa is unknown. It is possible that clay is lost to the system via lateral translocation and/or carried further downslope in the process of colluviation and thus contributes very little to the Terra Rossa.

Particle size distribution and chemistry

Both the Terra Rossa and Upslope profiles show increasing clay and silt from the A and B horizons relative to the coarser fractions. Given the lack of clay mobility evident in the micromorphological analysis it would be expected that there would be a relatively homogenous amount of clay throughout the profile. The high clay mobility in the Upslope profile and the greater proportions of clay in the B horizon than the A suggests illuviation. This illuviation of clay into the B horizon results in larger proportions of sand in the A horizon. This supports an allochthonous origin as the movement of material

from Upslope via creep may explain the unexpected increase in sand and silt sized particles in the A horizon of the Terra Rossa.

The amount of dolomite required to produce 40 cm of soil was calculated given that in MacLeod (1980) it was required that 130 m of 0.15% insoluble residue limestone be dissolved to produce a 40 cm profile. Only 3-4 m of the dolomite with 6.5% insoluble residue would need to be weathered to produce 40 cm of soil. This calculation assumes the bulk density of the soil and the dolomite are 1.3 g.cm^{-1} and 2.65 g.cm^{-1} respectively (MacLeod, 1980), as these data were not available. This implies that it would take approximately 1.5×10^5 years (Yaalon & Ganor, 1975) for 40 cm to develop. This suggests that an autochthonous explanation for the origin of the Terra Rossa is acceptable as it is not improbable that a soil should survive erosion for this length of time.

The $\text{Al}_2\text{O}_3:\text{K}_2\text{O}$ ratios (Figure 6b) of the Terra Rossa fine earth reveal a significant difference between the upper (A and B1) horizons and lower (B2 and C) horizons. The sudden decrease in K_2O between the B1 and B2 horizons correlates with XRD data suggesting the appearance of vermiculite in the lower horizons. Vermiculite is associated with the loss of K from the mica and replacement with Ca (Bassett, 1959). The $\text{K}_2\text{O}:\text{CaO}$ ratio (Figure 6c) suggests that K is dominant in the upper horizons while Ca increases in the lower horizons. If the Terra Rossa were solely autochthonous one would expect the Ca to be greater in relation to the K in the upper as well as the lower horizons as it is weathered out of the profile. The relatively larger amounts of K in the Upslope profile, a soil derived from a non-carbonaceous parent rock, suggests that the Terra Rossa is receiving contributions from upslope via soil creep that is diluting the Ca in the upper horizons, and is, at least in part, allochthonous.

The larger $\text{K}_2\text{O}:\text{SiO}_2$ ratios (Figure 6d) of the dolomite compared with the rest of the profile could be explained by weathering out of the K rich minerals relative to SiO_2 and/or contribution from upslope via creep of SiO_2 rich minerals. This is supported by the relatively large amounts of SiO_2 relative to K_2O in the A horizon of the upslope profile. The relatively high levels of K_2O in the clay fraction of the upslope A horizon suggests that it is the sand and silt sized particles contributing to the dilution of the Terra Rossa K_2O .

The $\text{Fe}_2\text{O}_3:\text{K}_2\text{O}$ ratios (Figure 6e) reveal a significant increase in Fe_2O_3 in the B2 and C horizons of the Terra Rossa. This is because the lack of K and abundance of Ca in the lower profile creates structure in the soil, allowing air and water flow thus encouraging the development of Fe-oxides. Higher up the profile, where K is prevalent, Fe_2O_3 is relatively less abundant suggesting contributions of high K, low

Ca from upslope. The Ca and Fe₂O₃ are still higher in the upper Terra Rossa profile than in the Upslope profile suggesting that the Ca moves up the profile from the dolomite into the A and B1 horizons. This is also shown in the morphological analysis in that strong structure is observed throughout the Terra Rossa. The Ca input from the dolomite provides explains why the Terra Rossa is observed as coincident with lithology, despite contributions from upslope. The Ca accounts for the structure throughout the profile, promoting the development of Fe-oxides (particularly haematite), giving the soil its characteristic red colour (Bronger, 1983; Torrent *et al.*, 1983; Torrent & Schwertmann, 1987; Boero & Schwertmann, 1989; Singer *et al.*, 1998), regardless of the contributions from upslope. The upslope profile may also be high in Fe, however, due to the lack of Ca and subsequent structure, goethite is formed preferentially to haematite and so remains brown (Boero & Schwertmann, 1989).

If the Terra Rossa was autochthonous one would expect that the TiO₂:Zr ratios (Figure 6f), being largely associated with very resilient minerals, to remain roughly the same from the dolomite right throughout the profile. This, however, is not the case. The variability of this ratio also suggests an allochthonous origin for the Terra Rossa profile.

Clay and silt mineralogy

The larger amounts of quartz and the smaller amounts of primary mica in the upper horizons of the Terra Rossa silt fraction are distinct from deeper in the profile. There are greater levels of mica compared to quartz in the dolomite and an obvious relationship with the B2 horizon by way of the mica-vermiculite association, and the similarly small amounts of quartz. The presence of vermiculite is indicative of the weathering of primary mica from the dolomite. Weathering of mica results in the release of K⁺ into the soil solution and the dissolution of the dolomite results in the release of Ca²⁺. Thus, the exchange of Ca²⁺ for K⁺ in the interlayer spaces of the clay will convert the mica into vermiculite (Bassett, 1959). In the A and B1 horizons no vermiculite is present and considerably larger amounts of quartz are found. This suggests perhaps an allochthonous origin for the upper horizons of the profile whereas closer to the dolomite the soil is largely autochthonous.

Analysis of the clay fraction also supports this view. Little to no quartz can be found in the dolomite and B2 horizon, whereas it is clearly present in the upper horizons.

The view of an allochthonous origin for the upper portion of the profile is further strengthened by the XRD traces from the texture contrast profile upslope. In the silt fraction it is clear that quartz and primary

mica are the dominant minerals, with quartz the more abundant. This is identical to the mineralogy of the A and B1 horizons of the Terra Rossa. Furthermore, the considerable levels of quartz in the clay fraction throughout the profile are similar to the upper horizons of the Terra Rossa profile; this implies that there has been some contribution of clay sized particles from Upslope.

Coarse particle morphology and elemental chemistry

The FESEM counts of quartz, mica and K feldspar from the coarse sand fraction deep in the Upslope profile show roughly equal proportions. Proportions change gradually such that quartz becomes dominant in the upper horizons (Table 4). This suggests that as the soil develops, the less resilient minerals (mica and K feldspar) weather out of the profile leaving relatively more quartz.

The insoluble residue from the underlying dolomite of the Terra Rossa has considerably more mica than the upslope profile. Similar results were observed in the B horizon, whereas the A horizon is clearly dominated by quartz of silt and fine sand size. One explanation is that perhaps the mica and feldspar have weathered out of the profile, leaving proportionately more quartz. There is, however, a lack of evidence for a much more chemically aggressive environment in the A horizon, relative to the B horizon, that would predispose mica and feldspar of silt and sand size to break down to such a degree and yet leave the quartz grains with similar morphology in the A horizon as the grains in lower horizons. Delgado *et al.* (2003) come to a similar conclusion: Terra Rossas have formed in a “relatively calm pedoenvironment”. A more likely explanation is that the upper horizon has received contributions from upslope, i.e. at least the A horizon of the soil is allochthonous in origin.

This is supported by the morphological analysis of the grains under the FESEM. The angular morphology of the quartz grains from the dolomite is not a feature that is seen throughout the Terra Rossa profile. Should the grains from the A and B horizon have been derived from the dolomite, angular, dissolution-scarred morphology should predominate (Figure 11e). Instead, subrounded to well-rounded quartz grains (Figure 11a & c), that show a striking resemblance to the grains from the upslope profile (Figure 11f, h & j), are dominant. The severe weathering required to round the grains to this degree are sedimentological processes, thus grains must have been weathered prior to deposition. It is highly improbable that the dissolution scarring of the quartz in the dolomite would disappear in the Terra Rossa soil environment. The most likely explanation is that, whereas the dolomite residue does contribute a minor amount of sand to the upper horizons, the major contribution of sand is from upslope. Other

external sources are possible. Aeolian deposition is a possibility but, if the contribution from this source were significant, it would have affected the whole landscape. The similarity in quartz grain morphology throughout the Upslope soil profile eliminates this as a likely source for all but a minor amount of silt and fine sand.

Conclusion

The results of the analytical, mineralogical and morphological studies lead to the conclusion that the Terra Rossa soil is partly autochthonous in origin, having inherited material from the underlying dolomite, and partly allochthonous. The external source is most likely silt and fine sand eroded from the A horizon of a Brown Chromosol soil upslope. The soil can, however, be regarded a lithomorphous soil as it is dependent on the Ca from the dolomite to give it the features unique to the Terra Rossa, i.e. porous, highly structured, red, medium-textured, shallow soils (Bronger, 1983).

References

- Bartelli, L.J. & Odell, R.T., 1960. Laboratory studies and genesis of a clay enriched horizon in the lowest part of the solum of some Brunizem and Gray-Brown Podzolic soils in Illinois. *Soil Society of America Proceedings*, **24**, 390-395.
- Bassett, W.A., 1959. Origin of the vermiculite deposit at Libby, Montana. *American Mineralogist*, **44**, 282-300.
- Boero, V. & Schwertmann, U., 1989. Iron oxide mineralogy of terra rossa and its genetic implications. *Geoderma*, **44**, 319-327.
- Bourman, R.P. & Alley, N.F., 1988. Permian glacial features, north western Fleurieu Peninsula, South Australia. *Quarterly Geological Notes of the Geological Survey of South Australia*, **108**, 2-6.
- Brewer, R., 1976. Fabric and Mineral Analysis of Soils, pp. 482. Krieger, New York.
- Brewer, R. & Sleeman, J.R., 1988. Soil Structure and Fabric, pp. 173. CSIRO, Melbourne.
- Bronger, A., 1983. Rubification of *Terrae Rossae* in Slovakia: A Mossbauer effect study. *Clays and Clay Minerals*, **31**, 269-276.
- Bronger, A. & Bruhn-Lobin, N. 1997. Palaeopedology of *Terrae rossae*-Rhodoxerals from Quaternary calcarenites in NW Morocco. *Catena*, **28**, 279-295.

- Commonwealth Bureau of Meteorology, 7 October 2003. Climate averages by number.
<www.bom.gov.au/climate/averages/tables/cw_023751.shtml.
- Delgado, R., Martin-Garcia, J.M., Oyonarte, C. & Delgado, G. 2003. Genesis of the *terrae rossae* of the Sierra Gador (Andalusia, Spain). *European Journal of Soil Science*, **54**, 1-16
- Dove, P.M. & Nix, C.J., 1997. Influence of the alkaline earth cations magnesium, calcium and barium on the dissolution kinetics of quartz. *Geochimica et Cosmochimica Acta*, **61**, 3329-3340.
- Firman, J.B., 1969. Quaternary period. In: L.W. Parkin (Editor), Handbook of South Australian Geology, pp. 204-233. Geological Survey of South Australia, Adelaide.
- Gal, M., 1967. Clay mineralogy in the study of the genesis of terra rossa and rendzina soil originating from calcareous rocks. *Proceedings of the International Clay Conference, Jerusalem, Israel, 1966*, **1**, 199-207.
- Isbell, R.F., 1996. The Australian Soil Classification, CSIRO, Melbourne.
- Kubiena, W.L., 1953. The Soil of Europe, 145 pp. Thomas Murby and Company, London.
- MacLeod, D.A., 1980. The origin of the Red Mediterranean soils in Epirus, Greece. *Journal of Soil Science*, **31**, 125-136.
- McDonald, R.C., Isbell, R.F., Speight, J.G., Walker, J. & Hopkins, M.S., 1984. Australian Soil and Land Survey Field Handbook, 160 pp. Inkata Press, Melbourne.
- McIntyre, D.S., 1956. The effect of free ferric oxide on the structure of some terra rossa and rendzina soils. *Journal of Soil Science*, **7**, 302-306.
- Moresi, M. & Mongelli, G., 1988. The relation between the terra rossa and the carbonate free residue of the underlying limestones and dolostones in Apulia, Italy. *Clay Minerals*, **23**, 439-446.
- Norrish, K. & Rogers, L.E.R., 1956. The mineralogy of some terra rossas and rendzinas of South Australia. *Journal of Soil Science*, **7**, 294-301.
- Preiss, W.V., 1987. The Adelaide Geosyncline - late proterozoic stratigraphy, sedimentology, palaeontology and tectonics, 438 pp. Bulletin of the Geological Society of South Australia, Adelaide.
- Rayment, G.E. & Higginson, F.R., 1992. Australian Laboratory Handbook of Soil and Water Chemical Methods. Australian Soil and Land Survey Handbooks, 3rd Edn, 330 pp. Inkata Press, Melbourne.
- Singer, A., Schwertmann, U. & Friedl, J., 1998. Iron oxide mineralogy of *terrae rossae* and rendzinas in relation to their moisture and temperature regimes. *European Journal of Soil Science*, **49**, 385-395.

- Soil Survey Staff, 1975. Soil Taxonomy: a basic system of soil classification for making and interpreting soil surveys. U.S. Department of Agriculture, Handbook No. 436, Washington DC.
- Stace, H.C.T., 1956. Chemical characteristics of terra rossas and rendzinas of South Australia. *Journal of Soil Science*, **7**, 280-293.
- Torrent, J., Schwertmann, U., Fechter, H. & Alferez, F., 1983. Quantitative relationships between soil color and hematite content. *Soil Science*, **136**, 354-358.
- Torrent, J. & Schwertmann, U., 1987. Influence of hematite on the color of red beds. *Journal of Sedimentary Petrology*, **57**, 682-686.
- Webb, B.P., 1957. Summary of tectonics and sedimentation. In: L.W. Parkin (Editor), The Geology of South Australia, pp. 136-148. Journal of the Geological Society of Australia.
- Wellman, P. & Greenhalgh, S.J., 1988. Flinders/Mount Lofty Ranges, South Australia; their uplift, erosion and relationship to crustal structure. *Transactions of the Royal Society of South Australia*, **112**, 11-19.
- Yaalon, D.H., 1997. Soils in the Mediterranean region: what makes them different? *Catena*, **28**, 157-169.
- Yaalon, D.H. & Ganor, E., 1975. Rates of aeolian dust accretion in the Mediterranean and desert fringe environments of Israel. *International Congress of Sedimentology, Nice*, **2**, 169-174.

Table 1 Properties of the fine earth and insoluble residue

Profile	Depth (cm)	Horizon	Particle Size Distribution (%)					CEC ^a	pH	EC ^b	Exchangeable Bases ^c			
			Clay	Silt	Very fine sand	Fine sand	Coarse sand				K	Na	Ca	Mg
Terra Rossa	0-10	A	40	27	22	6	5	12.1	6.20	0.45	0.8	1.4	22.6	3.8
	20-28	B	56	19	16	5	4	12.1	5.83	0.25	0.6	1.2	20	2.9
	40-47	B	74	12	10	2	2	15.0	5.88	0.23	0.8	1.4	20.4	3.5
	47-55	C	84	8	5	1	1	5.0	8.38	0.15	0.5	1.4	25.4	1.4
	>55 ^d	R	6	18	21	33	22	n/a	n/a	n/a	n/a	n/a	n/a	n/a
Upslope	0-10	A	28	30	28	9	4	8.5	5.57	0.28	0.7	1.0	14.8	3.0
	23-42	B	47	22	19	8	3	9.2	5.51	0.18	1.2	2.8	10	5.4
	42-63	B	54	20	18	5	2	11.1	5.83	0.14	1.2	1.4	11.4	7.3
	83-100	C	37	29	20	13	2	17.3	6.94	0.09	1.0	1.6	9.6	7.3
	>135 ^e	R	n/a	n/a	n/a	n/a	n/a	n/a	n/a	n/a	n/a	n/a	n/a	n/a

^aCation exchange capacity.^bElectrical conductivity.^cMeasured in milliequivalents.100g⁻¹.^dDolomite – values taken from insoluble residue.^eShale – values taken from ground rock.

Table 2 X-ray fractionation data for trace element analysis

Profile	Fraction	Depth	Trace Elements (ppm)																					
			Zr	Nb	Y	Sr	Rb	U	Th	Pb	Ga	Cu	Zn	Ni	Ba	Sc	Co	V	Ce	Nd	La	Cr	Mo	As
Terra Rossa	Clay	0-10cm	185.2	22.5	61.8	50.0	151.3	5.5	40.6	63.1	28.3	30	73	44	339	27.9	41	164	204	70	94	149	5	20
		20-28cm	184.7	14.4	155.5	37.9	134.6	3.8	41.0	52.4	30.3	13	52	48	253	29.6	35	170	260	154	155	158	4	20
		40-47cm	159.7	12.3	120.8	31.0	112.9	2.7	33.2	44.0	30.2	9	46	51	186	26.6	25	167	163	113	104	161	4	24
		47-55cm	163.0	9.6	10.8	22.6	88.9	4.2	28.1	15.5	24.3	8	39	33	106	18.9	10	107	34	8	12	105	3	17
	Whole Soil	0-10cm	272.4	18.1	78.4	72.7	111.2	3.0	22.6	31.6	16.7	10	33	22	459	17.7	22	106	161	83	89	98	1	10
		20-28cm	274.6	18.9	102.1	63.3	120.5	3.4	28.8	35.4	22.9	8	34	31	411	23.6	26	137	189	110	109	126	2	12
		40-47cm	214.7	14.0	98.8	46.9	112.9	3.3	30.0	37.7	26.6	5	36	42	303	24.0	22	152	159	101	96	150	2	20
		47-55cm	54.4	3.7	25.6	161.9	26.8	1.2	9.2	9.9	7.2	0	13	11	202	*	7	50	45	19	20	37	4	6
		Dolomite ^a	34.0	2.7	10.8	241.7	9.9	0.8	5.2	4.7	1.2	0	8	5	44	*	4	16	35	5	13	14	6	4
		Dolomite(IR) ^b	248.1	15.3	2.2	70.4	95.0	7.4	14.6	6.3	12.9	7	13	19	502	2.7	20	67	56	18	27	71	5	12
Upslope	Clay	0-10cm	143.5	28.6	16.2	72.8	251.6	4.5	33.7	57.6	21.8	30	86	26	505	19.6	14	123	120	41	72	136	4	14
		42-63cm	158.9	16.7	26.2	56.7	264.5	4.8	35.4	53.3	26.2	15	72	37	340	25.1	13	150	176	63	94	170	3	15
	Whole Soil	0-10cm	250.7	18.6	11.8	84.2	119.2	2.5	16.5	24.5	14.3	8	28	10	523	12.9	8	74	65	21	31	74	0	7
		42-63cm	238.7	20.1	19.6	73.9	192.5	3.4	23.8	36.7	19.8	7	46	22	509	21.2	8	119	129	44	66	128	1	9
		Siltstone	221.9	19.3	23.7	111.5	157.8	4.9	35.6	22.4	19.1	10	81	20	965	21.2	11	94	178	74	66	113	1	7

^aWhole dolomite, no acid treatment.^bDolomite insoluble residue.

Table 3 X-ray fractionation data for major element analysis

Profile	Fraction	Depth	Major Elements (%)											LOI ^a (%)	Total (%)
			SiO ₂	Al ₂ O ₃	Fe ₂ O ₃ T	MnO	MgO	CaO	Na ₂ O	K ₂ O	TiO ₂	P ₂ O ₅	SO ₃		
Terra Rossa	Clay	0-10cm	34.12	21.17	11.90	0.34	1.20	0.72	4.94	2.04	0.91	7.59	0.27	13.05	98.24
		20-28cm	35.51	23.63	13.40	0.20	0.98	0.95	3.34	1.58	0.93	4.96	0.08	13.08	98.64
		40-47cm	37.54	25.04	14.33	0.09	1.07	1.04	2.46	1.29	0.86	3.60	0.07	12.21	99.57
		47-55cm	36.11	18.17	9.75	0.01	0.95	1.12	8.43	0.95	0.79	11.92	0.05	9.81	98.06
	Whole Soil	0-10cm	60.98	13.65	6.06	0.16	0.79	0.85	0.34	2.88	0.84	0.21	0.04	12.81	99.59
		20-28cm	56.96	18.26	9.05	0.14	0.80	0.67	0.31	2.76	0.94	0.18	0.01	9.96	100.05
		40-47cm	48.42	22.35	11.87	0.08	1.06	0.98	0.25	2.11	0.91	0.27	0.01	11.45	99.75
		47-55cm	11.09	5.30	2.92	0.02	1.76	40.56	0.27	0.39	0.25	0.13	0.32	36.26	99.27
		Dolomite ^b	5.01	1.03	0.71	0.03	3.09	46.00	0.34	0.45	0.11	0.21	0.25	40.54	97.75
		Dolomite (IR) ^c	78.76	10.33	1.99	0.00	0.48	0.26	0.92	4.92	0.61	0.06	0.06	1.30	99.69
Upslope	Clay	0-10cm	34.93	16.69	7.16	0.17	2.63	1.17	6.89	3.36	0.99	10.40	0.34	13.25	97.98
		42-63cm	39.42	22.57	11.35	0.02	3.12	0.51	3.40	2.76	1.08	4.84	0.05	9.44	98.55
	Whole Soil	0-10cm	69.76	9.96	2.99	0.07	1.06	0.51	0.48	2.68	0.72	0.12	0.00	11.49	99.83
		42-63cm	60.00	17.35	7.36	0.01	2.31	0.35	0.32	3.21	0.95	0.04	0.01	7.59	99.48
		Siltstone	63.04	15.26	5.94	0.01	4.50	0.26	0.81	4.52	0.88	0.04	0.01	4.05	99.34

^aLoss on ignition.^bWhole dolomite, no acid treatment.^cDolomite insoluble residue.

Table 4 FESEM mineralogy counts of 125-2000 μm fraction

Profile	Depth	Mineral Type (%) ^a		
		Quartz	Mica	K Feldspar
Terra Rossa	0-10	65	32	3
	20-28	30	50	20
	Dolomite (IR)	38	61	1
Upslope	0-10	82	8	10
	42-63	70	18	12
	85-100	28	33	39

^aPercent calculated relative to each other.

Figure Captions

Figure 1

Sampling locality and regional distribution of the Terra Rossa and related geology.

Figure 2

Trench being dug for sampling (S 35° 33' 53.1", E 138° 11' 46.0").

Figure 3

Terra Rossa profile and soil morphology (S 35° 33' 53.1", E 138° 11' 46.0").

Figure 4

Upslope profile and soil morphology (S 35° 33' 49.5", E 138° 11' 43.9").

Figure 5

Depth plots of the (a) Terra Rossa and (b) Upslope profiles showing relative proportions of grain size fractions in the fine earth.

Figure 6a

Depth plot of the $\text{Al}_2\text{O}_3:\text{Fe}_2\text{O}_3$ ratio of the whole soil.

Figure 6b

Depth plot of the $\text{Al}_2\text{O}_3:\text{K}_2\text{O}$ ratio of the whole soil.

Figure 6c

Depth plot of the $\text{K}_2\text{O}:\text{CaO}$ ratio of the whole soil.

Figure 6d

Depth plot of the $\text{K}_2\text{O}:\text{SiO}_2$ ratio of the clay fraction and whole soil.

Figure 6e

Depth plot of the $\text{Fe}_2\text{O}_3:\text{K}_2\text{O}$ ratio of the whole soil.

Figure 6f

Depth plot of the $\text{TiO}_2:\text{Zr}$ ratio of the whole soil.

Figure 7

Mineralogy of the silt fraction (2-20 μm) of selected horizons of the (a) Terra Rossa and (b) upslope soils.

Figure 8

Mineralogy of the silt fraction (2-20 μm) in the region of 3-16°2 θ for the (a) Terra Rossa and (b) upslope soils.

Figure 9

Mineralogy of the clay fraction ($<2\mu\text{m}$) of the (a) Terra Rossa and (b) upslope soils.

Figure 10

Mineralogy of the clay fraction ($<2\mu\text{m}$) in the region of $3-16^\circ 2\theta$ for the (a) Terra Rossa and (b) upslope soils.

Figure 11

FESEM photographs of the coarse sand fraction ($125-2000\mu\text{m}$).

- (a) Subrounded quartz grain from the A horizon of the Terra Rossa. The surface is relatively smooth with some pits and grooves.
- (b) Hydrated mica from the B horizon of the Terra Rossa profile.
- (c) Subrounded quartz grains from the B horizon of the Terra Rossa. All show pits and grooves.
- (d) Primary mica crystal from the dolomite.
- (e) Angular quartz grain showing dissolution scars from the dolomite.
- (f) Well rounded quartz grain from the A horizon of the upslope profile.
- (g) Quartz and mica grains from the B horizon of the upslope profile. The quartz grain appears fresh.
- (h) Well rounded quartz grain from the B horizon of the upslope profile.
- (i) Mica from the C horizon of the upslope profile.
- (j) Subangular quartz grain from the C horizon of the upslope profile.

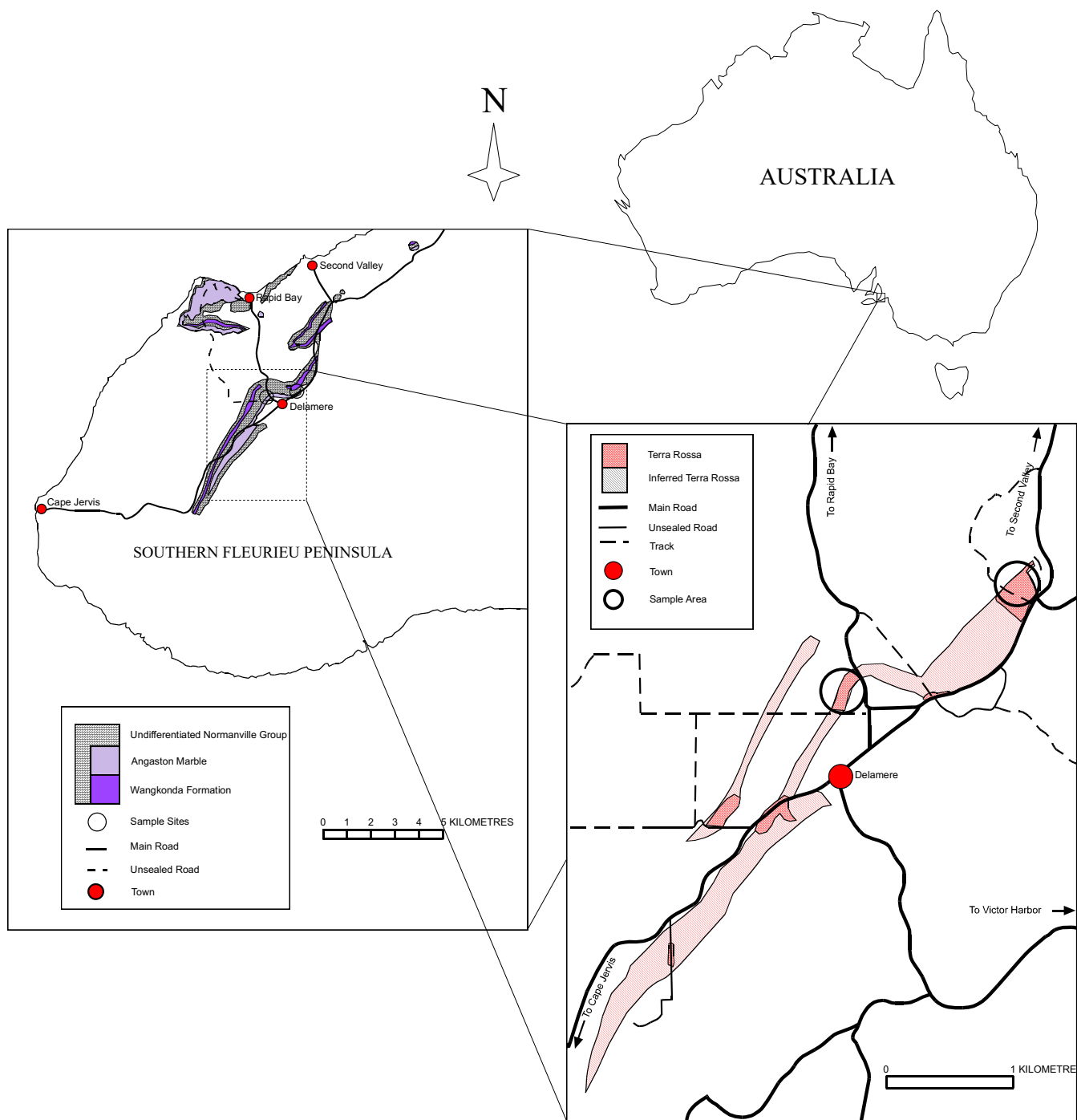


Figure 1



Figure 2

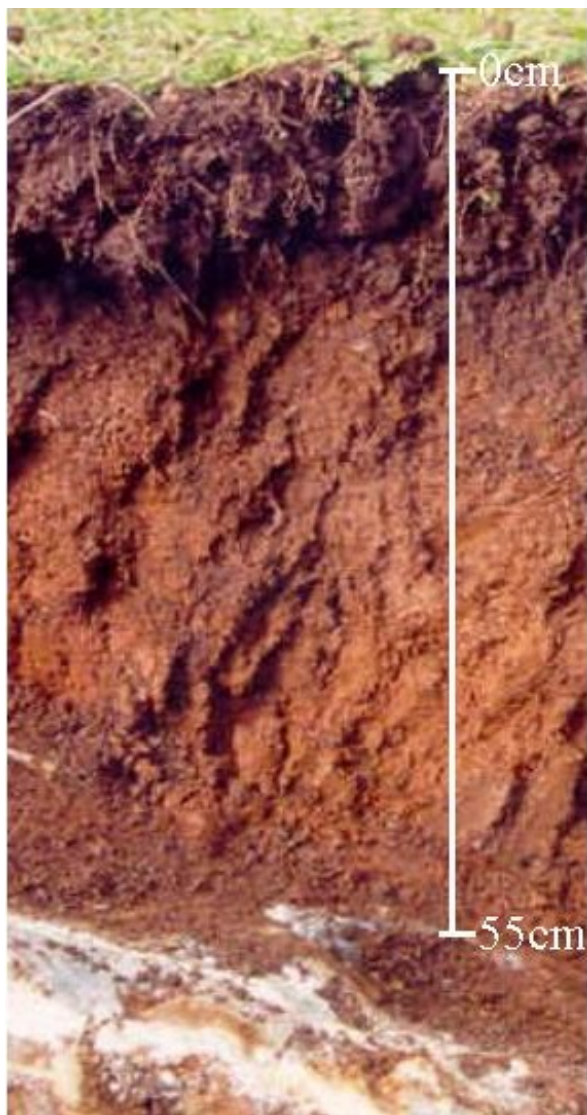


Figure 3

Depth (cm)	Horizon	Munsell Colour	Description
0-10	A	5YR 3/2	Loam; strong, granular structure.
10-20	A	5YR 3/2	Sandy clay loam; strong granular structure.
20-28	B	5YR 3/2	Clay loam; strong granular structure.
28-40	B	2.5YR 3/4	Clay loam; strong granular structure.
40-47	B	2.5YR 3/4	Clay loam; strong granular structure.
47-55	C	7.5YR 5/6	Sandy loam; very calcareous, no structure, weathered parent rock.
>55	R	n/a	Medium grained, crystalline dolomite.



Figure 4

Depth (cm)	Horizon	Munsell Colour	Description
0-10	A	5YR 3/1	Loam; moderate, granular structure.
10-23	A	7.5YR 2/2	Clay loam; moderate granular structure.
23-42	B	7.5YR 3/0	Light medium clay; moderate, subangular blocky structure.
42-63	B	7.5YR 2/0	Light clay; weak-moderate, subangular blocky structure.
63-85	B	10YR 5/6	Light clay; weak-moderate, subangular blocky structure.
85-100	C	10YR 6/4	Clay; weak, subangular blocky structure.
100-130	C	10YR 6/4	Sandy clay loam: massive structure.
130-135	C	10YR 6/4	Sandy loam; massive structure.
>135	R	n/a	Fine grained shale/siltstone.

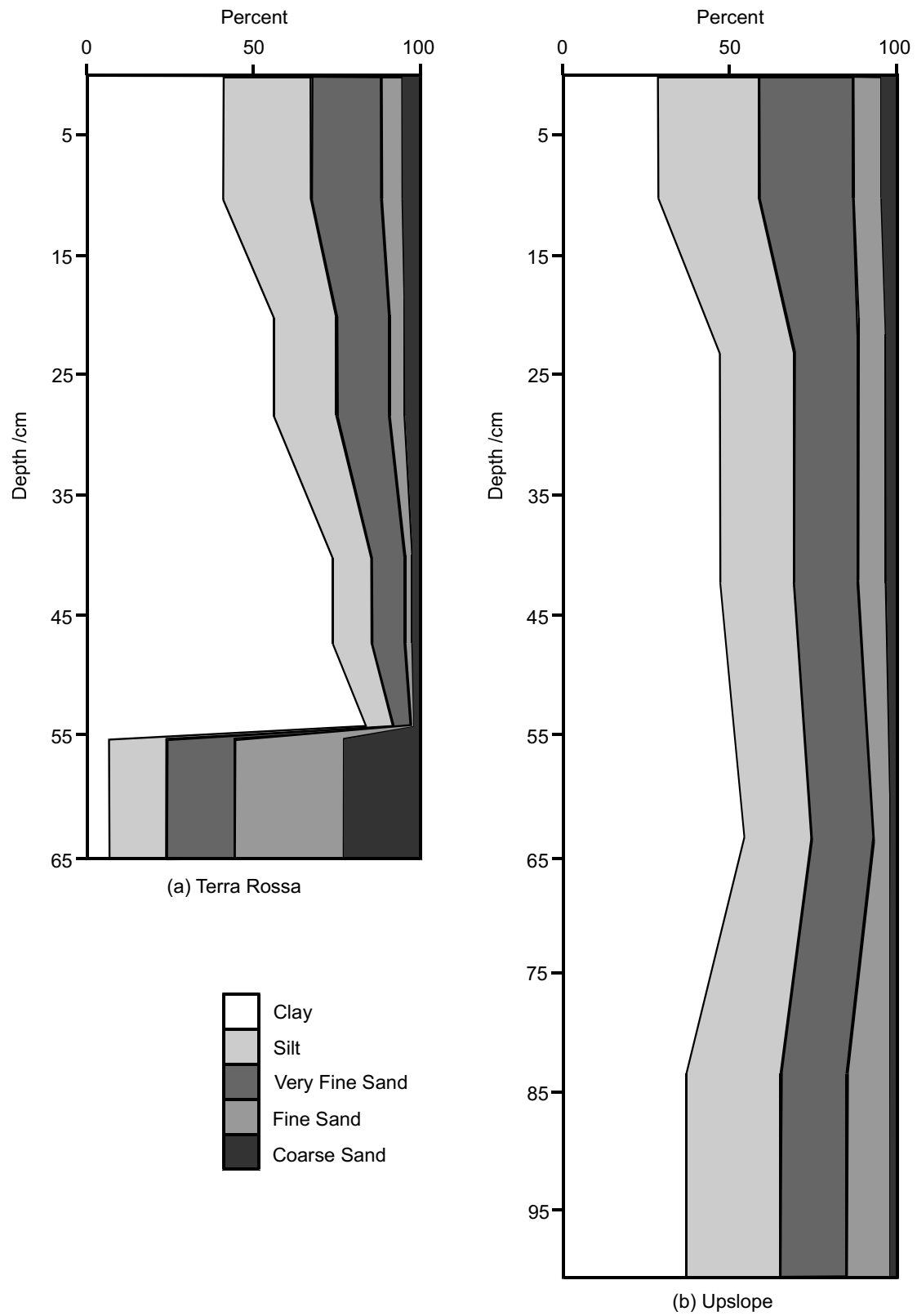


Figure 5

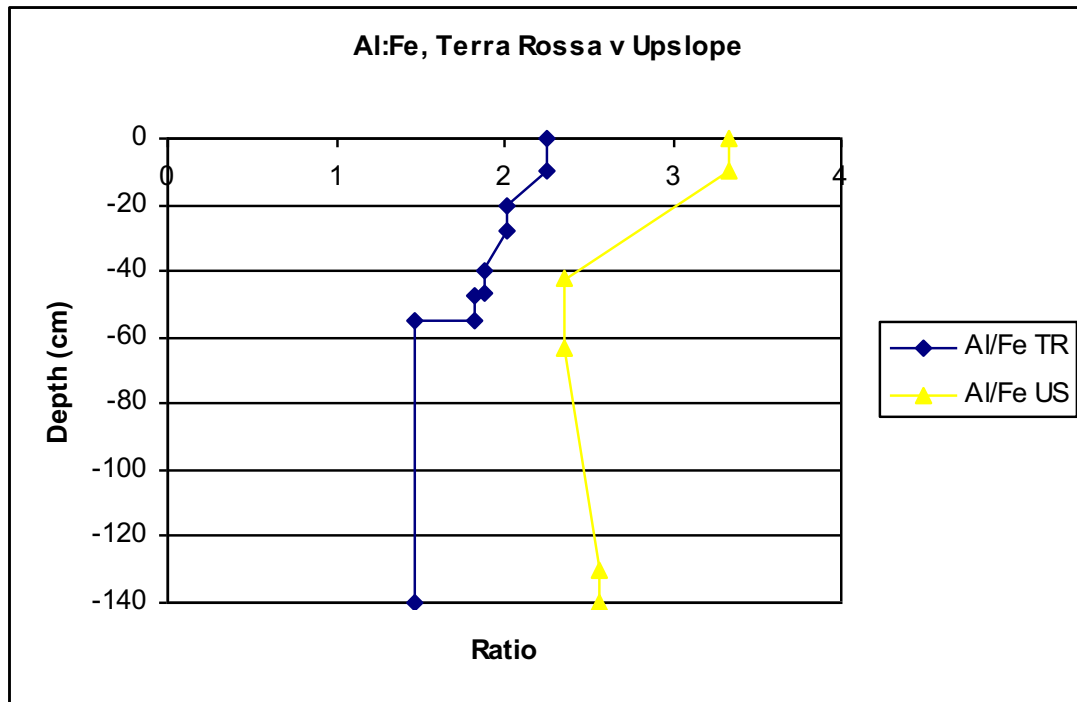


Figure 6a

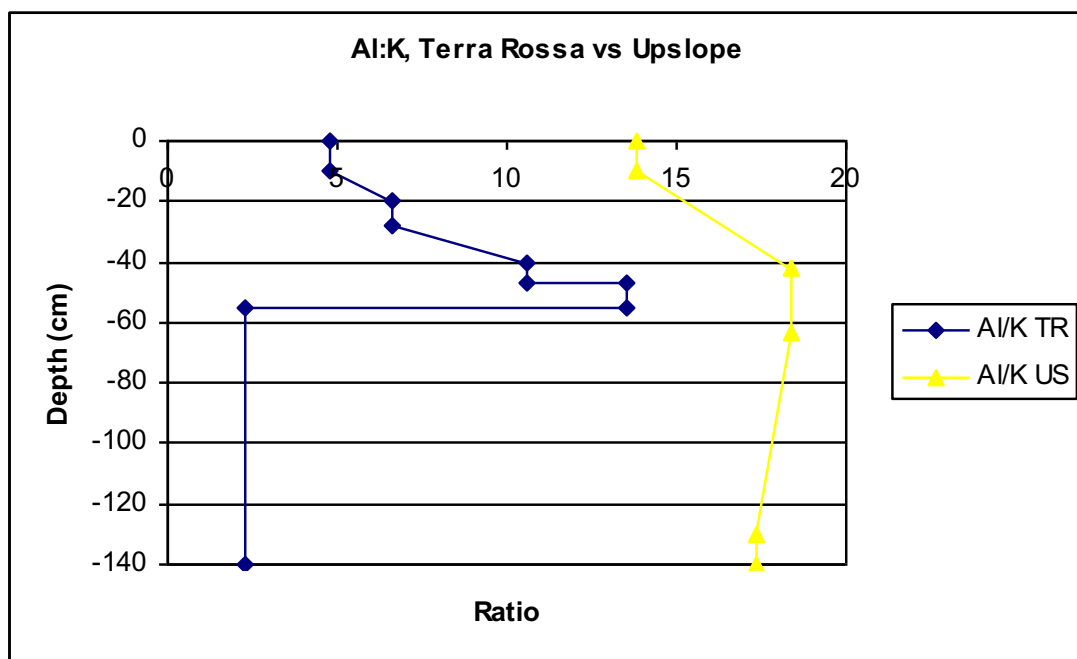


Figure 6b

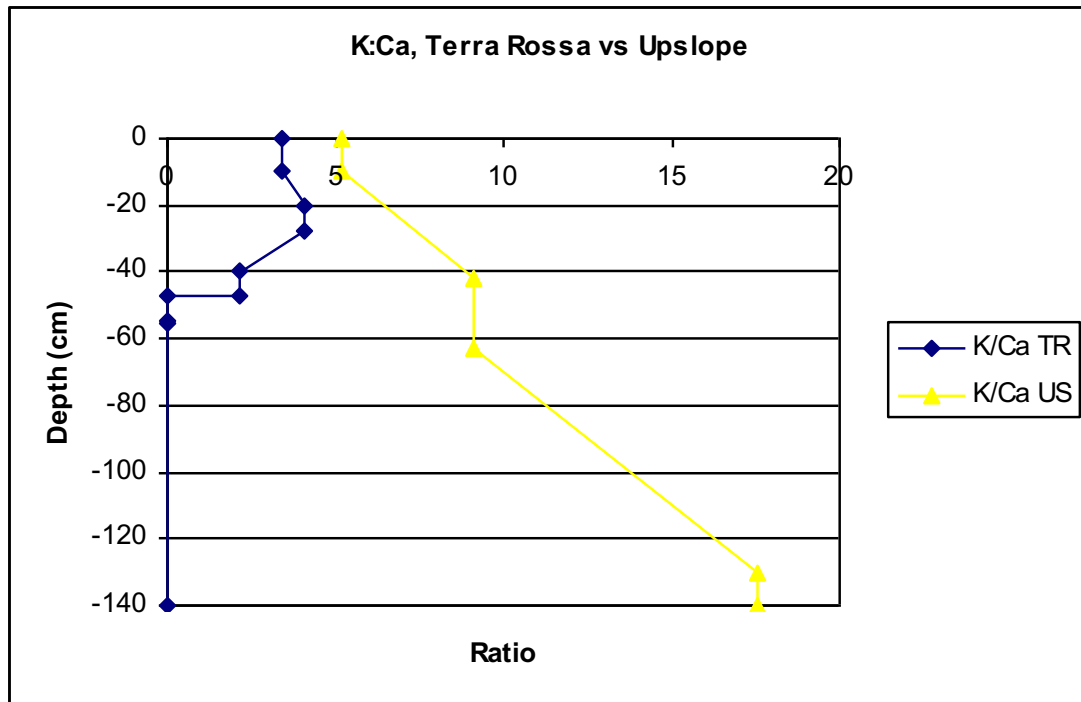


Figure 6c

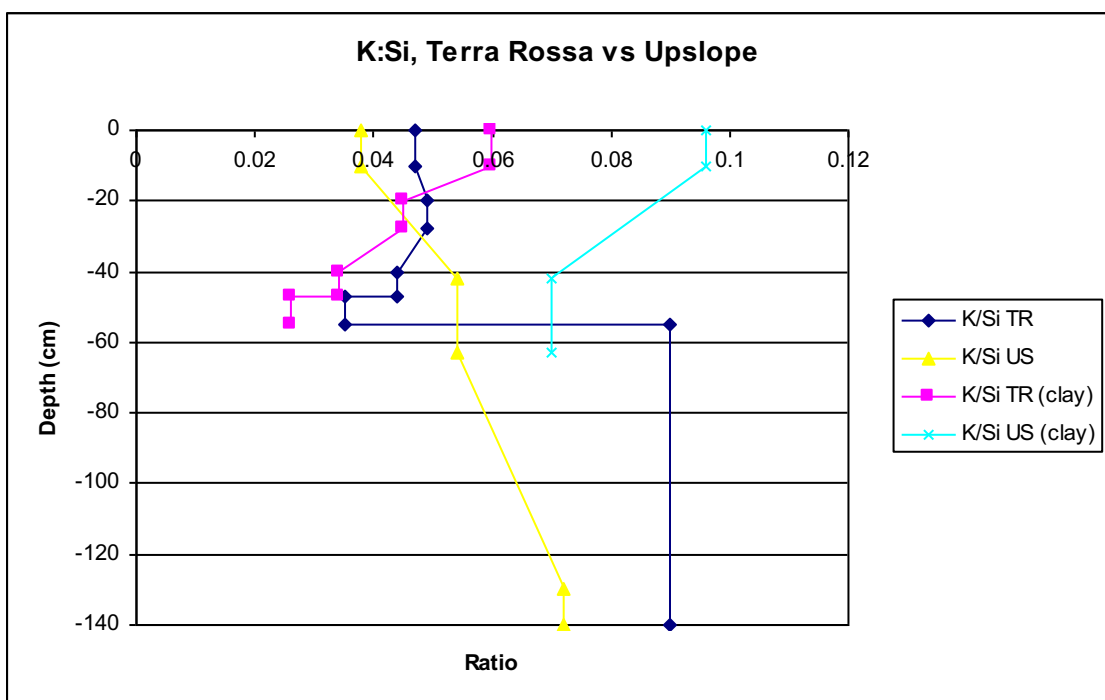


Figure 6d

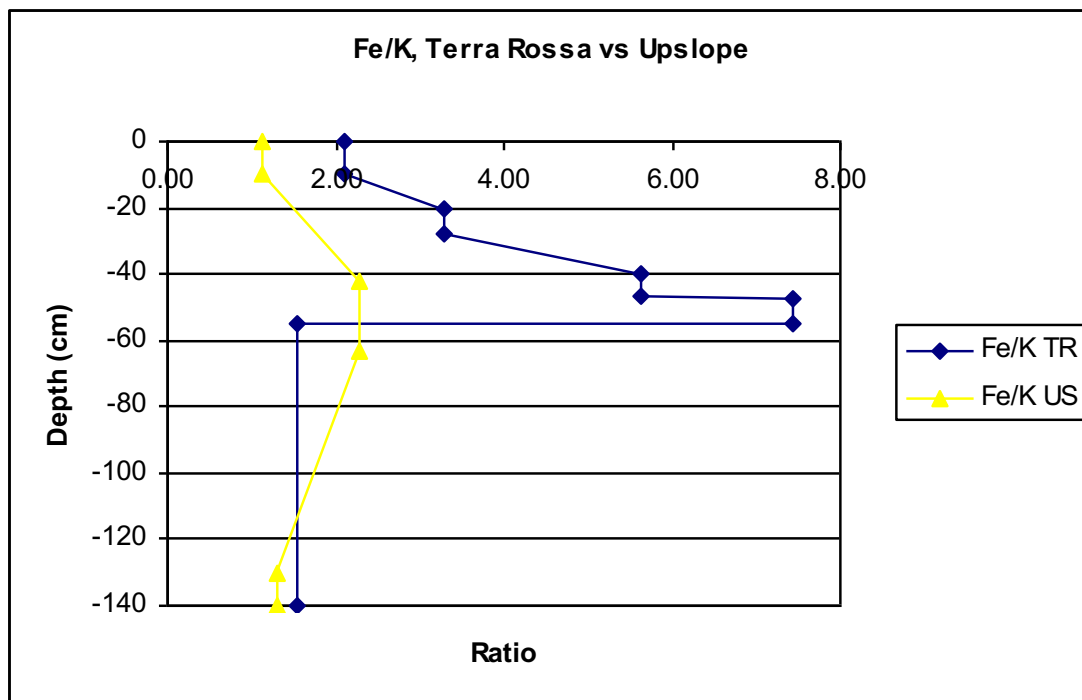


Figure 6e

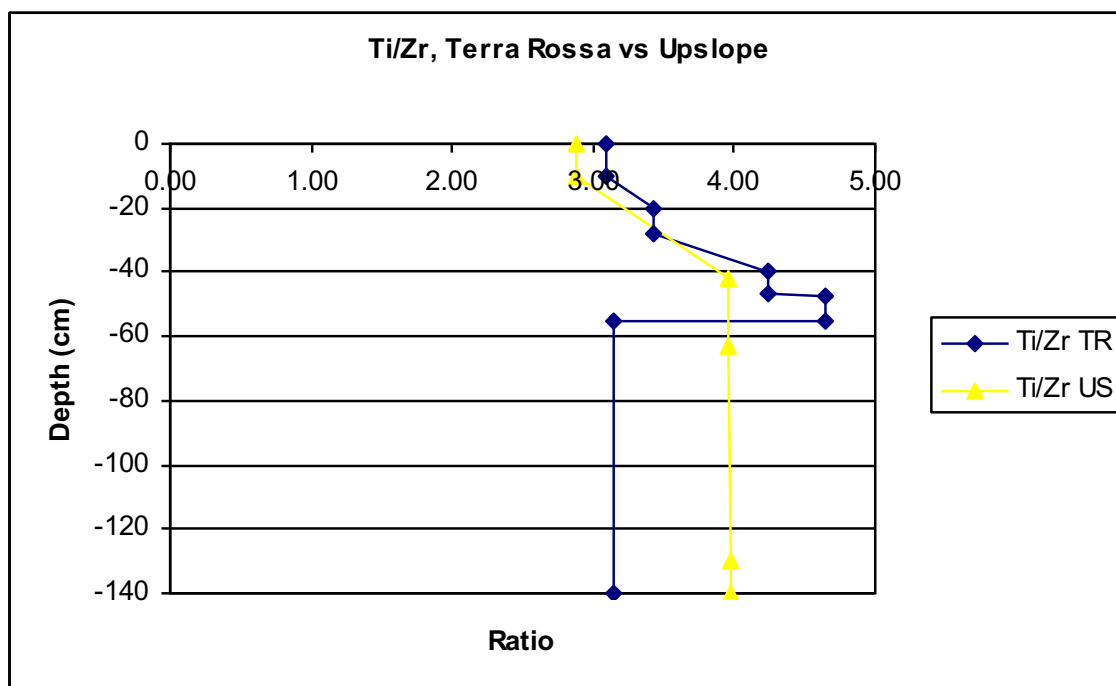


Figure 6f

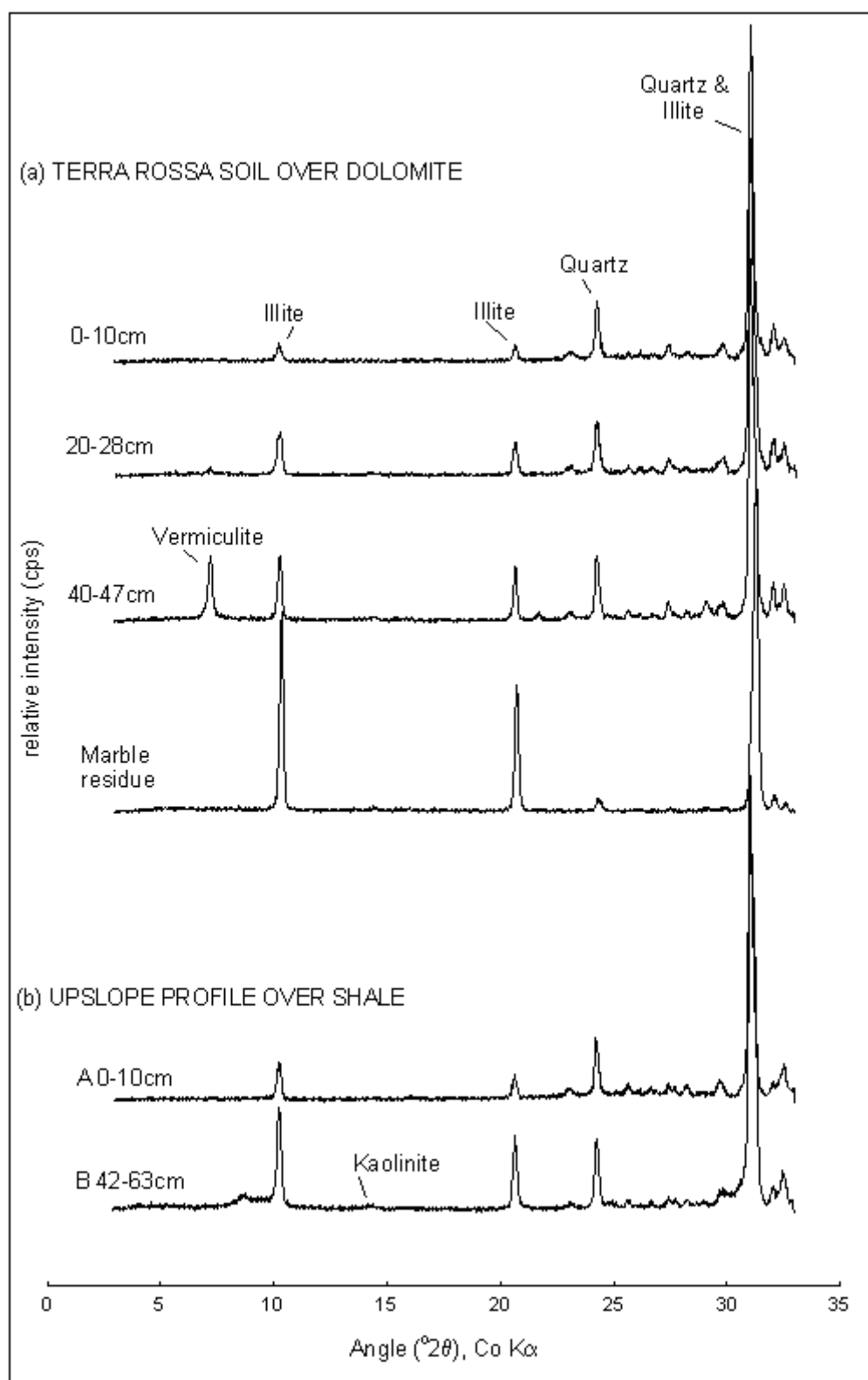


Figure 7

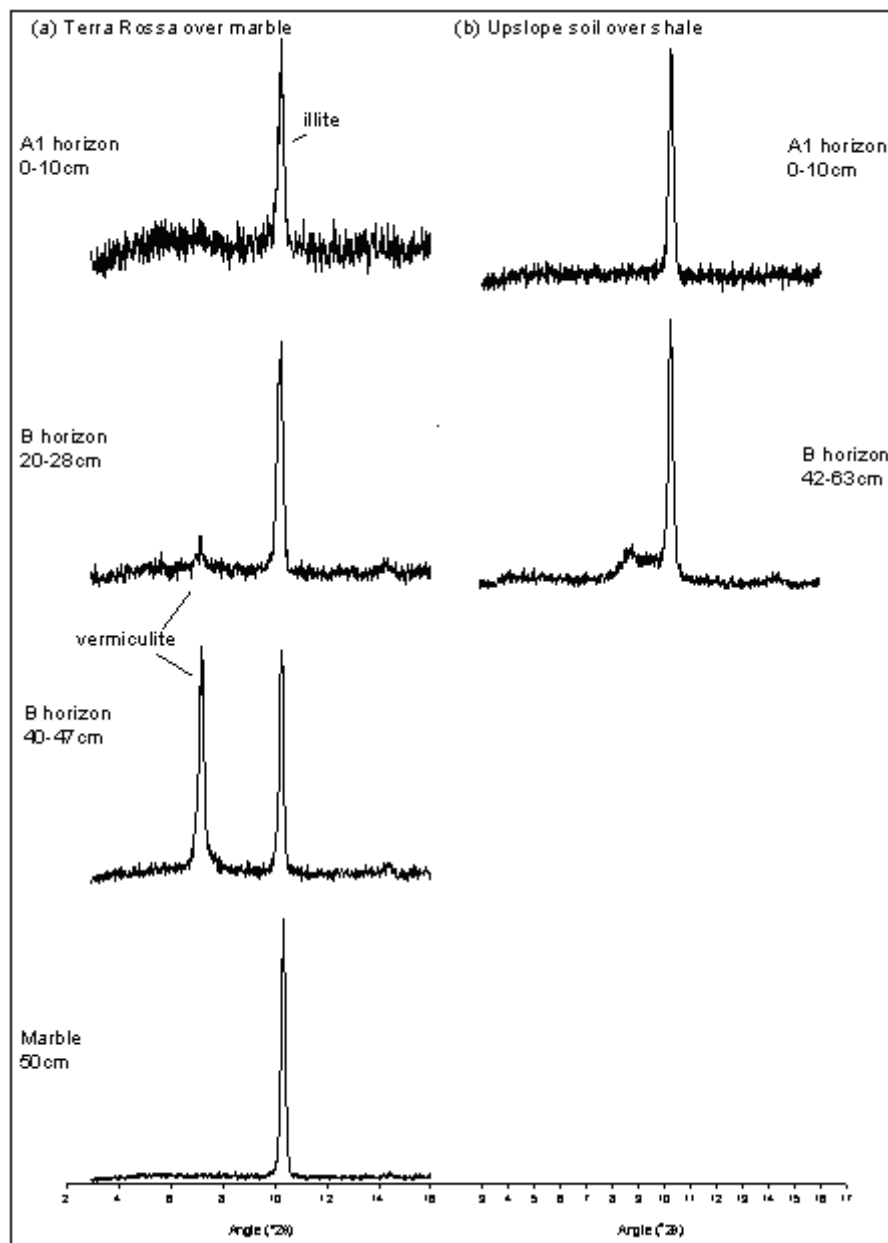


Figure 8

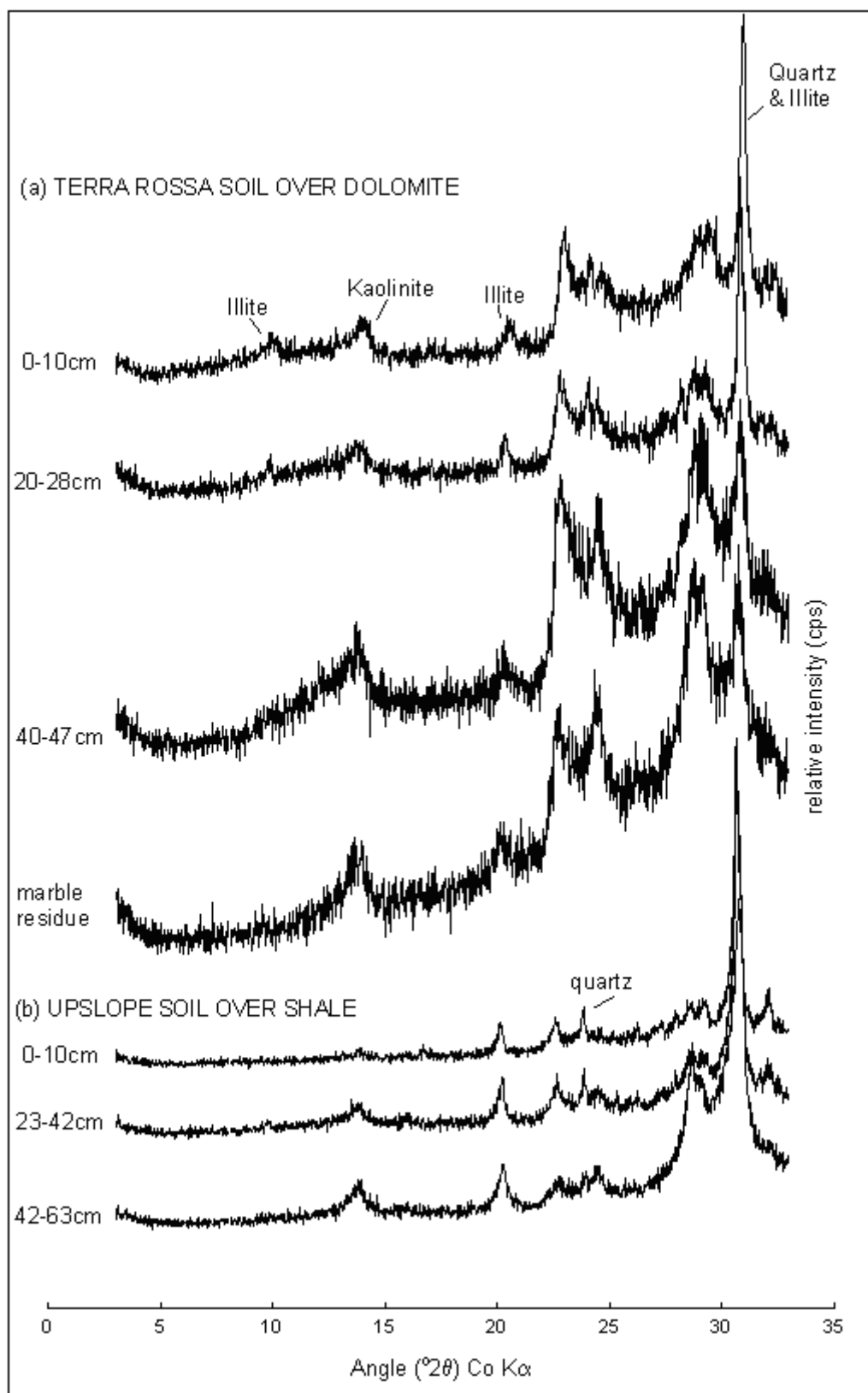


Figure 9

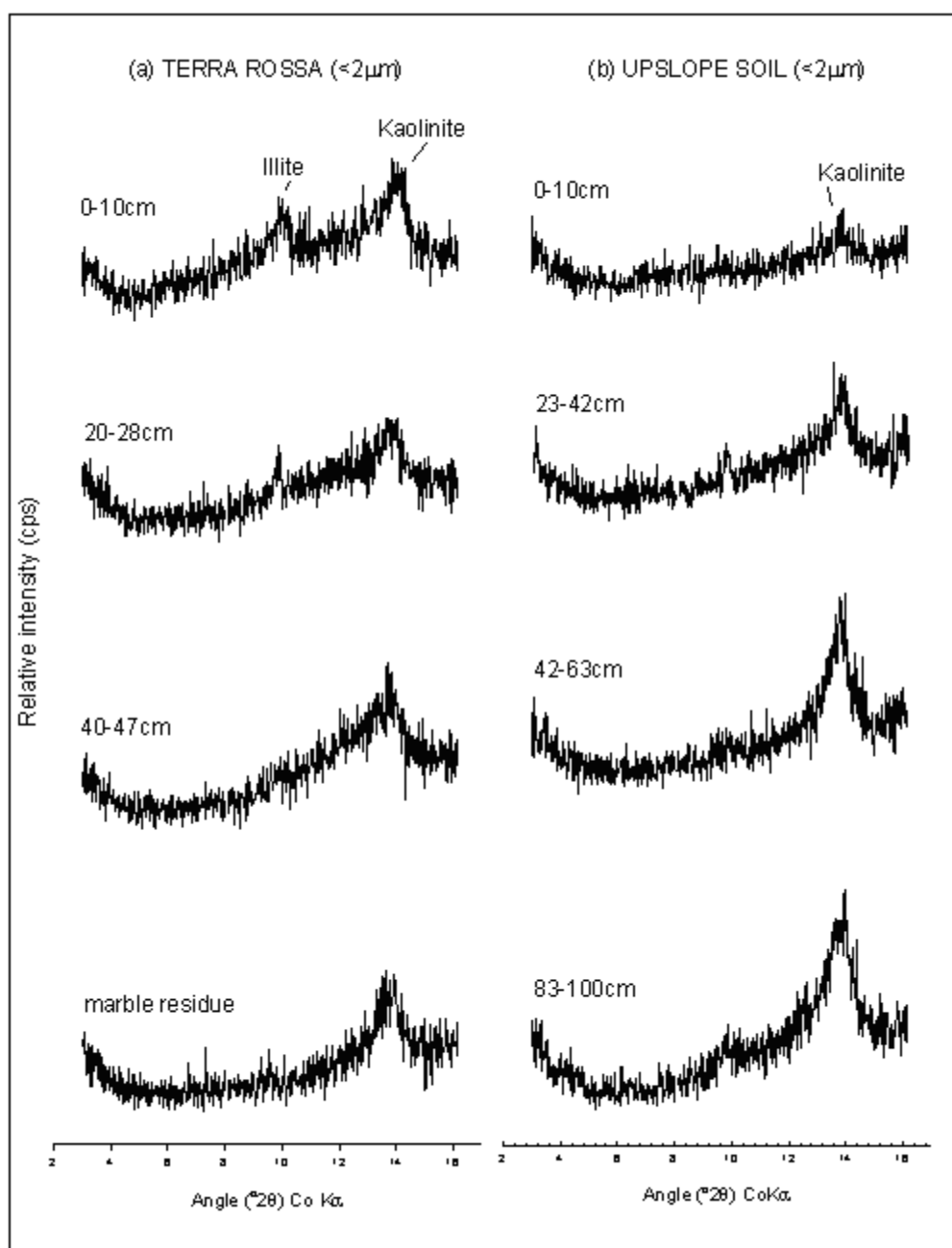
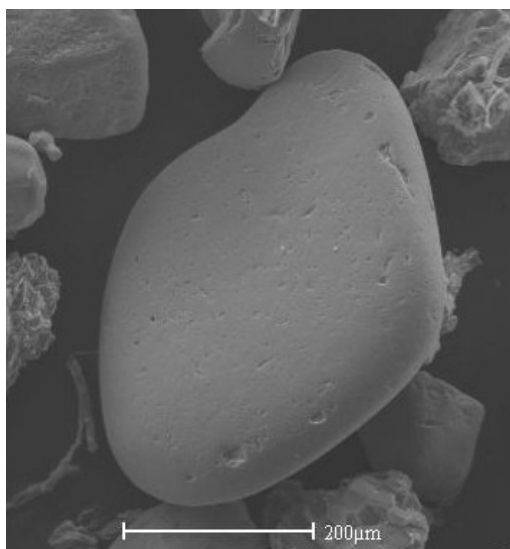
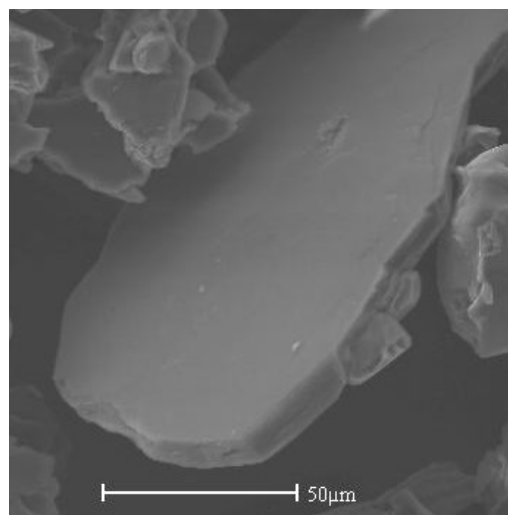


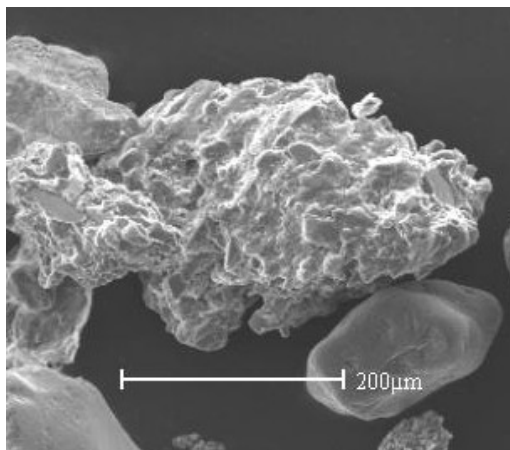
Figure 10



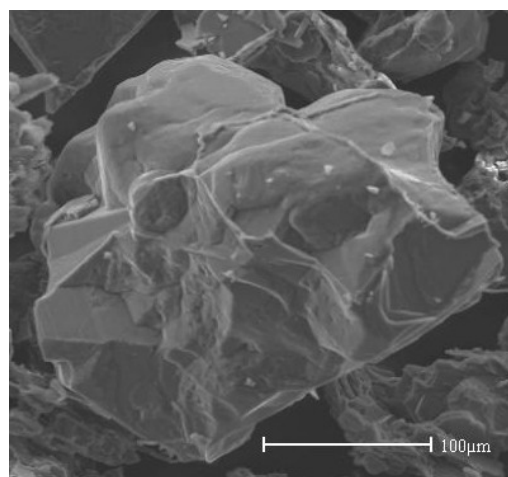
(a)



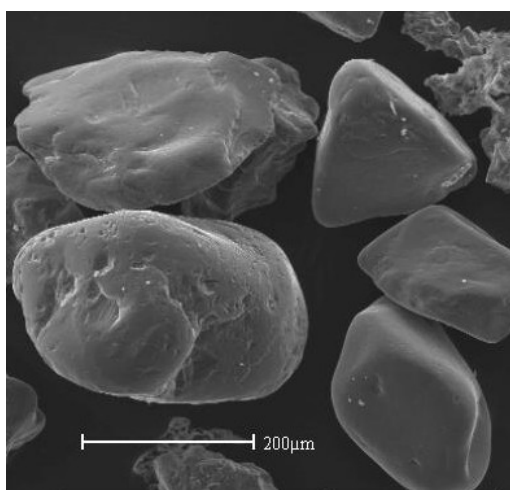
(d)



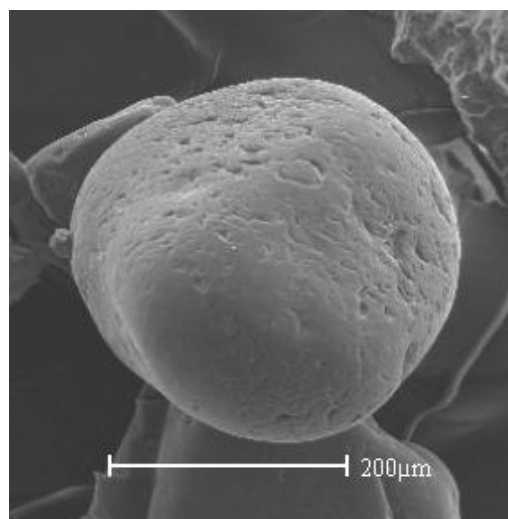
(b)



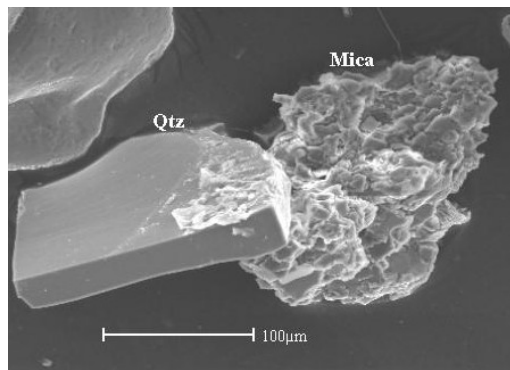
(e)



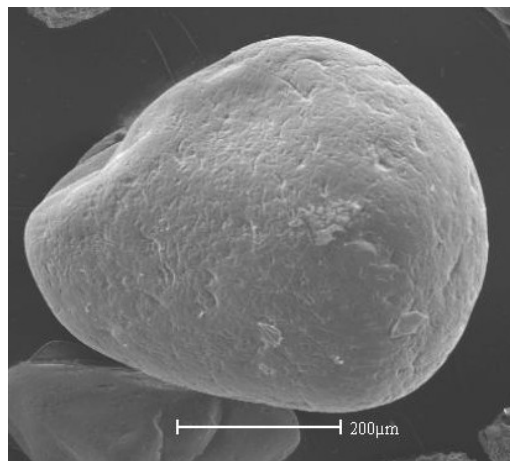
(c)



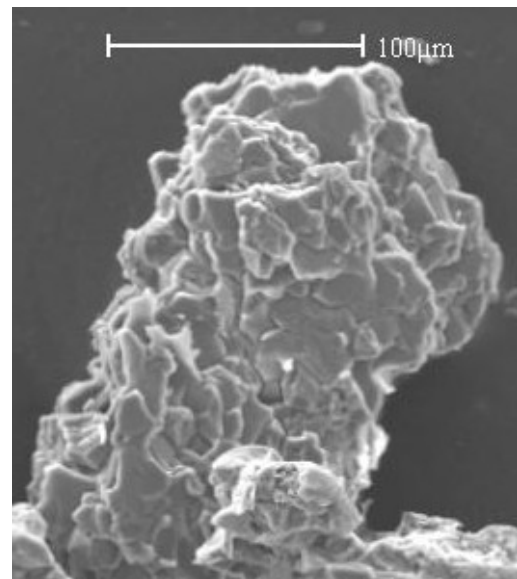
(f)



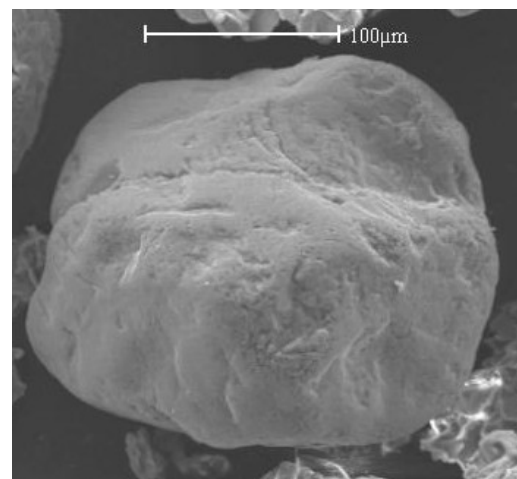
(g)



(h)



(i)



(j)

Figure 11